Journal of Luminescence 194 (2018) 316–320

Contents lists available at ScienceDirect

Journal of Luminescence

journal homepage: www.elsevier.com/locate/jlumin

Synthesis and fluorescence properties of lanthanide-supported titanate nanosheets

Daisuke Yoshioka[a,*], Yasumitsu Nishimura[b], Ken-ichi Katsumata[c,d]

[a] Department of Natural Sciences and Kawasaki Medical School, 577 Matsushima, Kurashiki, Okayama 701-0192, Japan
[b] Department of Hygiene, Kawasaki Medical School, 577 Matsushima, Kurashiki, Okayama 701-0192, Japan
[c] Materials & Structures Laboratory, Tokyo Institute of Technology, 4259 Nagatsuta-cho, Midori-ku, Yokohama, Kanagawa 226-8530, Japan
[d] Tokyo University of Science Photocatalysis International Research Center, 2641 Yamazaki, Noda, Chiba 278-8510, Japan

ARTICLE INFO

Keywords:
Photodeposition
Photoluminescence
Lanthanide
Titanate nanosheet

ABSTRACT

Metal oxide nanosheets are increasingly applied as catalysts, hard coatings, and other transparent thin film materials. Here, we developed a novel and appropriate photodeposition method for liquid-phase-synthesized titanate nanosheets (TNS). Lanthanide (Ln) oxide was suspended in the TNS dispersion, and the mixture was irradiated with UV light. Ln bearing on TNS (Ln/TNS) was easily achieved by this method. Eu/TNS, Sm/TNS, and Dy/TNS exhibited photoluminescence properties. In particular, Eu/TNS emitted strong red fluorescence under UV irradiation. Furthermore, the Ln/TNS retained the layered structure and diamond-like shape of TNS.

1. Introduction

Low-dimensional structures (nanotubes and nanosheets) have attracted attention for their potential utility in new technologies [1–4]. Because of their desirable characteristics, metal oxide nanosheets such as titanate nanosheets (TNS) are targeted as engineering, chemical and optical materials. A single nanosheet is composed of ultra-thin monocrystals (10^{-10}–10^{-8} m thick), and many nanosheets can be stacked to form a layered structure [1]. Identical or different nanosheets are easily stacked; furthermore, various molecules (such as dyes, metal cations, and organic molecules) can be intercalated within the layers [5–8]. Thus, metal oxide nanosheets and their derivatives are exploited as catalysts, photocatalysts, hard coats, and other functional transparent thin films [9–11]. The applications of nanosheets have diversified.

Many metal oxide nanosheets are synthesized by solid-phase methods, which require multiprocessing and are time consuming. In particular, high-temperature heating (800–1200 °C) and two long-term (2 weeks) stirrings are needed. Even over such long periods, large-size nanosheets tend to precipitate rather than disperse within the water. Recently, several groups have synthesized TNS by liquid-phase methods [1,12]. Aqueous TNS dispersion is easily obtained by a stirring process alone. The obtained TNSs are smaller than those of solid-phase-synthesized TNS and are much more dispersible in water. The liquid-phase-synthesized TNSs are uniform in size and shape and exhibit similar functions and characteristics to those of solid-phase-synthesized TNS [1,13], including the photocatalytic property.

Although liquid-phase-synthesized TNS has been recognized as photocatalytic, the bearing of metals on TNS by photodeposition has not been reported. Including metal cations in the solution might be problematic for two reasons. First, because both TNS and metal cations co-exist in liquid phase, the products and reactants would be difficult to separate. Second, the TNS surfaces are covered with a negative charge; therefore, the TNS and metal cations become flocculated by electrostatic interactions and subsequently precipitated [14,15]. We considered that these problems can be overcome by replacing metal ions with metal oxides in solution and exchanging the roles of the liquid and solid phases in the photodeposition method. By this approach, we aimed to develop new fluorescent nanosheets.

This study reports our reverse-phase photodeposition method using liquid-phase-synthesized TNS and lanthanide oxides and describes the mechanisms of bearing and emission of the synthesized Ln/TNSs.

2. Experimental section

2.1. Materials

Titantetrasiopropoxide, 10% tetraethylammonium hydroxide aqueous solution, 2-propanol, and acetone were purchased from Wako Pure Chemical Industries, Ltd, Osaka, Japan. and used as received. Arbitrary weights of lanthanide oxides (La_2O_3, CeO_2, Pr_6O_{11}, Nd_2O_3, Sm_2O_3,

Abbreviations: TNS, titanate nanosheet(s); Ln, lanthanoide; XRD, X-ray diffraction; TEM, transmission electron microscope; PL, photoluminescence

* Corresponding author.
E-mail address: d.yoshioka@med.kawasaki-m.ac.jp (D. Yoshioka).

http://dx.doi.org/10.1016/j.jlumin.2017.10.058
Received 12 September 2016; Received in revised form 19 October 2017; Accepted 20 October 2017
Available online 21 October 2017

Eu_2O_3, Gd_2O_3, Dy_2O_3, Ho_2O_3, Er_2O_3, Yb_2O_3, and Lu_2O_3) were also purchased from Wako. An arbitrary weight of Tb_2O_3 was purchased from Sigma–Aldrich, Co. LCC, St. Luis, Missouri, U.S.

2.2. Equipment for synthesis

Hydrothermal treatment was performed in a 4749 general purpose acid digestion vessel (autoclave vessel, Parr Instrumental Company, Moline, Illinois, U.S.). UV irradiation was supplied by a UVGL-25 (UVP, LLC, Upland, California, U.S.).

2.3. Equipment for evaluation

X-ray diffraction (XRD) patterns were obtained from D8 Discover (Bruker AXS K.K., Yokohama, Japan). Samples were dried and washed for XRD by a standard method. Transmission electron microscopic (TEM) observation was performed under a JEM-1400 (JEOL, Tokyo, Japan). The TEM samples were prepared by dropping the dispersion onto a micro grid or a mesh grid (Cu). The fluorescence spectra of the dispersions were obtained by an F-2700 instrument (Hitachi High-Tech Science Corporation, Tokyo, Japan).

2.4. Synthesis of titanate nanosheets

TNSs were synthesized from titantetraisopropoxide and tetraethylammonium hydroxide by the liquid-phase method [1,12]. The TNS dispersion was then transferred to the autoclave vessel. To grow the particles, the TNSs were heated to 110 °C for 6 h in an oil bath. After two heating processes, we obtained TNSs dispersed in an aqueous solution. The TNSs were observed and characterized by XRD, Raman spectroscopy, and Transmission Electron Microscopy.

Europium oxide (Eu_2O_3) powders were suspended in TNS dispersion and UV-irradiated for 30 min in the presence of Eu_2O_3. Following irradiation, the non-reacted Eu_2O_3 was removed and the irradiated dispersion was dried in air. The dried TNSs were washed with acetone and redissolved in water. Thus dispersed Eu^{3+} on TNS (Eu/TNS) was obtained. Both TNS and Eu/TNS dispersions formed colloids without precipitation during the long term observation. Other Ln/TNSs also were obtained in the same way.

3. Results and discussion

3.1. Eu^{3+} bearing on the liquid-phase-synthesized TNS

In this study, we implemented a novel photodeposition method for liquid-phase-synthesized TNS (see experimental Sections 2–4).

The Eu/TNS dispersion emitted red fluorescence when re-irradiated with UV (see Fig. 1). For a detailed investigation, we compared the fluorescence spectra of Eu/TNS with that of Eu_2O_3 in nitric solution. Both spectra are shown in Fig. 2(a). Comparing the emission and excitation peaks of these spectra, we find that the emission peaks of Eu/TNS, occurring at 590 nm and 615 nm, correspond to the f–f transition of Eu^{3+}, while the excitation peak at 310 nm is assignable to TNS absorption. Similar results were obtained for Eu^{3+}-intercalated TNS [14]. The ratio of the intensities at 590 nm and 615 nm indicates the

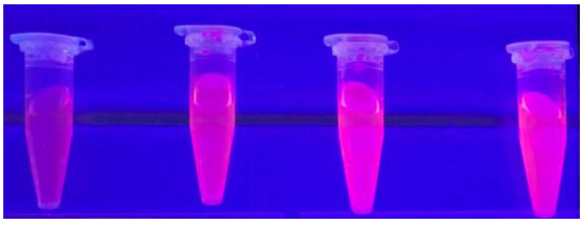

Fig. 1. Eu/TNS dispersion exposed to UV light.

symmetry around Eu^{3+}. The lower the symmetry around Eu^{3+}, the stronger the intensity at 615 nm [16]. In the present Eu/TNS fluorescence emission spectrum, the relatively strong peak at 615 nm indicates that the Eu^{3+} was positioned in asymmetric surroundings.

The XRD patterns of TNS and Eu/TNS are shown in Fig. 3. The peaks at low angles (2θ = 4–15°) indicate layering of the TNS and Eu/TNS compounds. The Eu/TNS peaks appear at an angle lower than that of the TNS peaks, suggesting that the inter-layer distance was widened from 0.63 nm in TNS to 1.01 nm in Eu/TNS. Moreover, the XRD pattern of Eu/TNS differs from that of TNS intercalated with Eu^{3+} [14], whereas the TEM images of TNS and Eu/TNS are almost identical (Fig. 4). Together, the XRD patterns and TEM images indicate that the shape and layered structure of TNS is preserved in Eu/TNS.

3.2. Mechanism of the Eu^{3+} bearing reaction

Our proposed photodeposition method differs from conventional methods. In the conventional method, the carrier (e.g., titania) and the metal ion (e.g., Ag^+) exist in solid and liquid phases, respectively. In this study, the liquid and solid phases were the carrier TNS and the metal oxide Eu_2O_3, respectively. The carrier needed to be phase-separated from the metal ions because liquid-phase-synthesized TNS is highly dispersible in water and reacts with metal ions. By reversing the phases of the carrier and metal ions, we suppressed the flocculation and facilitated Eu bearing to the TNS.

TNS possesses photocatalyst properties similar to those of titania. Thus, we propose a mechanism for the photodeposition of TNS (Scheme 1), based on the conventional photodepositon method using titania carrier (Scheme 2). UV-irradiation excites the electrons from the valence band (V.B.) to the conduction band (C.B.), inducing a redox reaction at the carrier surface (regardless of whether the carrier is TNS or titania). In the case of TNS, the excited C.B. electrons reduce one part of Eu_2O_3 (reduced-Eu_2O_3) while the holes in the V.B. reoxidize the reduced-Eu_2O_3. In this way, the Eu_2O_3 deposits onto the TNS surface. In the case of titania, the C.B. electrons reduce silver ions at the titania surface.

3.3. Other lanthanide cases

We applied our method to the oxides of other lanthanides (excluding Pm), yielding 13 Ln/TNS species. With one exception, the XRD patterns of the Ln/TNSs were very similar to those of Eu/TNS (see Fig. 3), and their interlayer distances were extended to 1.01 nm. The exception was Tb/TNS, whose interlayer distance remained that of the original TNS.

Similar to Eu/TNS, Sm/TNS and Dy/TNS exhibited the photoluminescence (PL) property. The fluorescence spectra of these TNSs are shown in panels (b) and (c), respectively, of Fig. 2. However, the fluorescence intensities of Sm/TNS and Dy/TNS were too weak to be observed by eye. The remaining Ln/TNS demonstrated no PL properties (as an example, the PL spectrum of Tb/TNS is shown in Fig. 2(d)). The excitation peaks of Sm/TNS and Dy/TNS derive from TNS (310 nm) and from the lanthanide oxides (about 400 nm). The emission peaks are consistent with the f–f transitions of Sm^{3+} and Dy^{3+}, respectively. These trends are similar to those of Eu/TNS. Clearly, TNS absorbed the UV energy and transferred its excited energy to Sm^{3+}, Eu^{3+}, or Dy^{3+}.

The XRD pattern and fluorescence spectrum of Tb/TNS differs from those of Sm/-, Eu/-, and Dy/TNS, suggesting that reversed-phase photodeposition did not convey Tb^{3+} ions to the TNS surface. In the mechanism mentioned above, whether the Ln^{3+} was borne onto TNS was determined by reduction and subsequent reoxidation processes of Ln_2O_3. The redox potentials of $Ln^{3+} + e^- \rightarrow Ln^{2+}$ and $Ln^{4+} + e^- \rightarrow Ln^{3+}$ are listed in Table 1 [16]. Eu^{3+} and Sm^{3+} are easily reduced to Ln^{2+} because of their lower potential than other Ln^{3+}. Gd^{3+}, Tb^{3+}, and Dy^{3+} are reduced only under a high electron voltage. Furthermore, Tb^{3+} readily oxidizes to Tb^{4+} because its oxidizing potential is the